



Università di Pisa
Facoltà di Medicina e Chirurgia
Scuola di Specializzazione in Radiodiagnostica

Direttore: Prof. Carlo Bartolozzi

Tesi di Specializzazione

*Evaluation of pelvic lymph nodes in patients with prostate cancer:
the role of Diffusion Weighted MR Imaging (DW-MRI)*

Relatore:
Chiar.mo Prof. Carlo Bartolozzi

Candidato: Dott.ssa Valentina Vallini

Anno Accademico 2010/2011

INDEX

| | |
|-----------------------------|-----------|
| Abstract | 3 |
| Introduction | 6 |
| Purpose | 9 |
| Patients and Methods | 9 |
| Results | 13 |
| Conclusion | 15 |
| References | 22 |
| Tables | 26 |
| Figures | 35 |

Abstract

PURPOSE: To evaluate the role of Diffusion-Weighted MR Imaging (DW-MRI) in the detection of pelvic lymph node metastases in patients with prostate cancer (PC) candidate to radical prostatectomy and extended pelvic lymph node dissection.

MATERIALS AND METHODS: From June 2011 to March 2012, 5 patients (median age: 67,2 years; range 56-76 years) with prostate cancer (high/intermediate risk patients, according to D'Amico Risk Groups), underwent MRI before surgical treatment using a 3T device and a 8 channel phased-array surface body coil. Imaging protocol included T2-weighted FSE, T1-weighted FSE and DWI sequence (b-values: 0, 500, 800, 1000 and 1500 s/mm²). The appearance of benign and metastatic lymph nodes on the FSE MR images was analyzed by two observers in conference. The measurement of the ADC value was performed by another radiologist, in the following nodal stations: proximal and distal external iliac, proximal and distal internal iliac and obturator, each on both right and left sides.

RESULTS: A total of 84 lymph nodes were removed during surgery (median: 16,8 lymph nodes per patient, range: 12 – 23 per patient) and histologically analysed. A total of 46 nodal stations underwent surgical resection and histopathological examination. The smallest metastatic lymph node detected by this method measured 4mm on its short axis. The appearance of benign and metastatic lymph nodes on the FSE MR images was

documented in terms of short axis, the long to short axis ratio, node contour and intranodal heterogeneity signal intensity, in all ten nodal stations. For each of these parameters a grading score system was assigned using a two-point-level score and the grade system was obtained by adding the point-level obtained for each of these 4 parameters. The Grading Score ranged from 4, indicator of a benign nature, to 8, with 8 having the worst score indicator of malignant nature. The mean Grading Score was $6,46 \pm 0,42$ in the nodal metastatic group and $5,02 \pm 0,59$ in the nodal non-metastatic group ($P < 0.0001$). A Grading Score > 4 was considered suspicious for malignancy.

With the threshold score of 4, the lymph node station-based sensitivity, specificity, positive and negative predictive values and diagnostic accuracy for FSE-MRI analysis, were 100%, 19%, 29%, 100% and 39%, respectively.

Mean ADC value was $0.796 \pm 0,09 \times 10^{-3} \text{ mm}^2 / \text{s}$ in the nodal metastatic group and $1,17 \pm 0,25 \times 10^{-3} \text{ mm}^2 / \text{s}$ in the nodal non-metastatic group ($P = 0.0008$).

The ADC cut-off value, obtained by the ROC curve was $0.91 \times 10^{-3} \text{ mm}^2 / \text{s}$.

Lymph node stations-based sensitivity, specificity, PPV, NPV and diagnostic accuracy for DW analysis, were 100%, 95,2%, 87,5%, 100% and 96,4%, respectively.

CONCLUSIONS: Our preliminary data seem to suggest that DW-MRI of lymph nodes can now be performed as part of a primary tumour staging without significantly increasing the imaging time. This unique modality can help to distinguish benign from

malignant lymph nodes and is more accurate than FSE-MRI evaluation alone. Further, large scale studies are certainly needed to confirm our initial results.

Introduction

The presence of pelvic lymph node (LN) metastases in patients with prostate cancer (PC) is of major relevance and is decisive for treatment planning.

Currently, pelvic lymph node dissection (PLND) represents the most accurate and reliable staging procedure for the detection of lymph node invasion in PC, but not all patients are at the same risk of harbouring pelvic LN metastases [1]. The radical prostatectomy with the pelvic lymph node dissection, represents a time consuming and relatively expensive procedure that requires inpatient hospitalization and restricted activity during a period of postoperative recovery. It is also associated with potentially early postoperative complications (bleeding, infections and lymphocele) and late postoperative complications (urinary incontinence, erectile deficit, anastomotic stenosis). For this reason, non-invasive imaging is important to streamline surgical resection protocol and it might be of great help in selecting patients who are suitable for PLND.

Certainly, the ideal imaging modality should fulfil some key criteria including accuracy, reproducibility, availability, cost effectiveness and efficiency. Unfortunately, none of the standard preoperative radiologic techniques available to date includes all of these parameters and the presence of lymph node metastases and thus prediction of nodal malignancy remains one of the most important challenges in treatment and prognosis of patients with PC. Until now, LN staging is routinely performed by conventional cross-

sectional imaging such as computed tomography (CT) and it is based on their morphological appearances, such as nodal size, with a threshold of 10 mm in short axis diameter or clusters of smaller regional LNs, the long to short axis ratio, borders (lobulated or spiculated), extracapsular spread and abnormal internal architecture (such as central necrosis) [2]. Some innovative techniques have been introduced in order to overcome this clinically significant staging problem.

Diffusion-weighted MR is a non-invasive imaging technique that yields tissue diffusion properties, thereby providing structural information on the underlying tissue. It has shown a high sensitivity and specificity for the detection and characterization of LN metastases of head and neck cancers [3] and it has been recently introduced as a promising technique for pelvic neoplasm, with only preliminary experience in PC.

DW-MRI aims to study the random thermal motion of water molecules (Brownian motion), and this is generally limited in neoplastic tissues because of the high cell density and abundance of intra- and inter-cellular membranes.

The mobility is then quantified by calculating the apparent diffusion coefficient (ADC).

Conventionally, restricted diffusion in areas of high cellular density (e.g. tumours) exhibits low ADC values compared with less densely cellular areas in which higher ADC values are exhibited. But at the qualitative analysis, the brightness of lymph nodes on high b-value images must not be misdiagnosed because also reactive nodal

hyperplasia can result in increased cellularity and can exhibit a range of high signal intensities on DW-MRI.

In clinical practice, DW-MRI of the lymph nodes is performed using at least two or more b-values. A high b-value is applied to eliminate background signal to make the cellular lymph nodes more conspicuous [4]. Metastatic lymph nodes often have increased cellularity density and consequently lower ADC; although, some metastatic disease can result in central nodal necrosis and ADC increase. Reduced ADC values may be also observed in fibrosis.

Therefore, using quantitative ADC evaluation, pre-surgical assessment based on ADC threshold values may be valuable, but must be interpreted with caution given the varying cut-off values for malignancy published in the literature. Moreover, necrotic areas and inflammatory nodal hyperplasia accompanied by increased cellularity and nodal heterogeneity remain limitations when ADC values are applied to characterize nodal disease. However, DW-MRI appears to be a promising, non-invasive technique to detect pelvic LN metastases even in normal sized LN [2].

Purpose

The aim of our study was to evaluate the feasibility and accuracy of preoperative DW-MRI for detection of pelvic metastatic lymph nodes in a cohort of patients with PC who were selected for radical prostatectomy (RP) and pelvic lymph node dissection (PLND).

Patients and Methods

Between June 2011 and March 2012, 5 consecutive patients (median age: 67,2 years; range 56-76 years) with histologically proven PC (high or intermediate risk patients, according to D'Amico Risk Groups, Table 1) and scheduled for RP and PLND, underwent DW-MRI before surgery.

Exclusion criteria:

- bone metastases on bone scan;
- previous treatment for PC;
- previous/concomitant malignancy;
- contraindications to MRI.

All patients were examined on a 3T MRI unit (DISCOVERY MR750; GE Healthcare) and a phase array surface coil (8 channel; gradient field strength 50 mT/m; slew rate 200 T/m/s) focused on the inferior abdomen was used. The entire pelvis, from the aortic

bifurcation to the pubic symphysis, was studied by application of the following sequences: breath-hold, fast spin echo (FSE) T1-weighted sequence (TR 600-800 ms, TE 6-7 ms, slice section 4 mm, spacing 0,4 mm) acquired in the transverse plain; breath-hold, FSE T2-weighted sequence (TR 5000-8000 ms, TE 80-85 ms, slice section 4mm, spacing 0,4 mm) acquired in the transverse plain; breath-hold, 3D T2 acquired in the transverse plain (TR 2000 ms, TE 90-93 ms, slice section 2,20 mm, spacing 1,10 mm); DW sequences (single-shot spin-echo echo-planar imaging), acquired with respiratory gating in the transverse plain, using multiple b-values sequence (b-values: 0, 500, 800, 1000 and 1500 s/mm²) (repetition time automatically adapted to the patient's breathing pattern, 3500-9200 ms, TE 65-69 ms, slice section 4 mm, spacing 0,4 mm, Nex 4). Acquisition time for the whole examination ranged from 30 to 40 min; DWI multiple b-values acquisition lasted no more than 6 min.

The lymph nodes were noted on an anatomic landmark chart divided into ten different anatomic regions (external iliac proximal and distal, internal iliac proximal and distal and obturator, each on both right and left sides).

All patients underwent radical prostatectomy with extended lymphadenectomy, inclusive of the ten different nodal stations in 3 patients. In 2 patients internal iliac proximal and distal on both right and left sides, were not removed due to intraoperative difficulties. In one patients the lymphadenectomy also included the common iliac right station.

Pelvic LNs were submitted separately for pathologic assessment according to their anatomic location and underwent a thorough pathologic examination in order not to miss any metastatic deposit. A pathologist with more than 15 years of experience in urogenital pathology was responsible for performing all pathological examinations. The pathologist received an anatomical chart recording the dissected nodal stations. If no nodes were found, the entire tissue underwent histopathological examination. Conventional MR images were read at the time of patient inclusion. The radiologist was blinded to histopathological findings and the pathologist was blinded to DW-MRI results.

The appearance of benign and metastatic lymph nodes on the FSE MR images was analyzed by two observers in conference in terms of short axis, the long to short axis ratio, node contour and intranodal heterogeneity signal intensity (evaluated on T2-weighted images), in all ten nodal stations. For each of these parameters, a Grading Score system (Table 2) was assigned, using a two-point-level score and the grade system was obtained by adding the point-level obtained for each of these 4 parameters: short axis ≤ 10 mm (point 1), short axis > 10 mm (point 2), the long to short axis ratio ≥ 2 (point 1), the long to short axis ratio < 2 (point 2), regular node contour (point 1), irregular node contour (point 2), intranodal homogeneous signal intensity (point 1), intranodal heterogeneous signal intensity (point 2). The Grading Score ranged from 4,

indicator of a benign nature, to 8, with 8 having the worst score indicator of a malignant nature.

The ADC measurements were performed by another radiologist expert in DWI of the abdomen. The reviewer included only nodal stations that showed a minimum of one node with a long axis greater than 4 mm, in order to reduce the effect of partial volume artefacts. A region of interest (ROI) as larger as possible inside the lymph node was utilized. The ADC values of LNs were calculated by multiple b-values sequence combining 0, 500, 800, 1000 and 1500 s/mm².

Statistical Analysis

For each patient ($n = 5$) and each pelvic side ($n = 28$) the Student's t test was used to compare the ADC value measured in the nodal stations in which a metastatic node was detected upon histopathological analysis ($n = 7$) and in the nodal stations in which non-metastatic nodes were detected upon histopathological analysis ($n = 21$). The Student's t test was also used to compare the Grading Score calculated in the nodal metastatic group and in the nodal non-metastatic group.

Results were considered to be significant with $P < 0.05$. To evaluate the diagnostic performance of the ADC in differentiating metastatic from non metastatic lymph nodes, the receiver operating characteristic (ROC) curve analysis was performed. From the

ROC curve, the optimal threshold, the value that showed the best separation between metastatic and non-metastatic lymph nodes, was extracted.

The sensitivity, specificity, positive predictive value (PPV), and negative predictive value (NPV) and diagnostic accuracy, were calculated for DW and FSE-MRI analysis.

Results

All patients ($n = 5$) well tolerated the MRI examination. A total of 84 lymph nodes were removed during surgery (median: 16,8 lymph nodes per patient, range: 12–23 per patient) and histologically analysed. A total of 46 nodal stations underwent surgical resection and histopathological examination. On DW-MRI only 53 lymph nodes and 28 nodal stations were evaluated, since only nodes with long axis > 4 mm were included in the image analysis (Table 3).

Demographic and biometric information are summarized in Table 4.

Two of 5 patients (prevalence 40%) had lymph node metastases in 7 of 28 nodal stations.

The mean Grading Score was $6,46 \pm 0,42$ (range, 6-7) in the nodal metastatic group and $5,02 \pm 0,59$ (range 4-6) in the nodal non-metastatic group ($P < 0.0001$) (Table 5) but a Grading Score = 4 (highly indicator of a benign nature) was found in only 4/21 nodal stations of the nodal non-metastatic group; the last 17 nodal stations showed a Grading Score > 4 . A Grading Score > 4 was considered suspicious for malignancy. In the nodal

metastatic group, all nodal stations showed a Grading Score ≥ 6 . With the threshold score of 4, the lymph node station-based sensitivity, specificity, positive and negative predictive values and diagnostic accuracy for FSE-MRI analysis, were 100%, 19%, 29%, 100% and 39%, respectively.

All of the lymph nodes in the nodal metastatic group, detected with FSE MR imaging, were < 10 mm in their short axis. The lymph node mean diameter (short axis) in the nodal metastatic group and in the nodal non-metastatic group was respectively $6,35 \pm 1,54$ mm (4-9mm) and $5,08 \pm 1,32$ mm (3-13,5mm). One patient had one benign lymph nodes larger than 10 mm (13,5mm) in its short axis.

For each lymph node at least 3 measurements were made and the lowest ADC value recorded was chosen. The mean ADC value was $0.796 \pm 0,09 \times 10^{-3}$ mm² /s in the nodal metastatic group and $1.17 \pm 0,25 \times 10^{-3}$ mm² /s in the nodal non-metastatic group (P = 0.0008) (Table 6).

The area under the ROC curve indicating the difference between metastatic and non-metastatic lymph node values was 0.96 (Table 7).

The ADC threshold value, obtained from the ROC curve to show the clearest separation between metastatic and non-metastatic lymph nodes, was 0.91×10^{-3} mm² /s; accordingly, an ADC equal to or less than 0.91×10^{-3} mm² /s was considered to be a metastatic lymph node (Table 8, 9).

With the threshold value from the ROC curve, the lymph node station-based sensitivity, specificity, positive and negative predictive values and diagnostic accuracy for DW analysis, were 100%, 95,2%, 87.5%, 100% and 96,4%, respectively.

Examples of benign and malignant lymph nodes evaluation are reported on Figures 1, 2 and 3.

Discussion

The assessment of prostate nodal metastases remains a difficult task and the extent of pelvic lymph node dissection (limited vs extended) and the most suitable candidates for this procedure are still a matter of intense debate. Preoperative detection of lymph node metastases in patients with prostate cancer is crucial for selection of the appropriate treatment strategy and thus for patient prognosis. Some authors base their decision with regard to the need for PLND on preoperative nomograms based mainly on routinely available preoperative variables [5-7]. This clearly allows identification of those patients for whom routine staging PLND might be omitted. Others favour performing PLND in all patients who are candidates for radical prostatectomy, regardless of baseline tumour characteristics [8]. This option is clearly associated with higher staging accuracy, especially if an extended template is adopted. Nevertheless, the staging benefit is balanced by the risk of exposing a certain number of patients to significant and potentially unnecessary PLND-related complications. The conventional cross-sectional

imaging such as computed tomography (CT) can not accurately differentiate between benign and malignant lymph nodes, especially in smaller size nodes (5-10mm) so that smaller metastases often go undetected. Reported CT sensitivity for the detection of lymph node metastases in the range of about 35% [9]. Similarly, standard MRI, dynamic contrast-enhanced MRI and even magnetic resonance spectroscopic imaging have shown no advantage over CT to predict the presence of LN infiltration [10-11]. Indeed, recent studies have shown that meticulous lymph node dissection in patients with PC discloses a high rate of metastases up to 25% in patients with preoperatively negative standard imaging studies [12]. Usually, pelvic nodes greater than 10 mm in the maximum short axis diameter are considered metastatic [13-14].

The ^{18}F -FDG (the most extensively used tracer in PET imaging) has shown low sensitivity in identifying prostate cancer, and its physiological urinary excretion reduces specificity in the staging of loco-regional disease. ^{11}C -choline tracer accumulates in the membranes of both normal and abnormal prostate cells and then the use of PET with choline, is limited to the evaluation of patients undergoing radical prostatectomy [15]. Therefore, ^{11}C -choline positron emission tomography (PET) has been investigated with inconclusive results.

Single photon emission CT fused with CT or MRI allowed a more precise localization of $^{99\text{m}}\text{Tc}$ -containing lymph nodes by improving spatial resolution and orientation in one study [16]. Although this modality appears promising, it is time-consuming,

expensive and dependent on the skills of the nuclear medicine specialist [17]. In addition, technetium uptake can be compromised in bulky nodal disease, in which over one third of positive nodes remain unidentified [16].

The use of lymphotropic ultrasmall superparamagnetic particles of iron oxide (USPIO) as a contrast agent for MRI has also been recently evaluated. In a study including 80 men with clinically localized PC, this technique was shown to increase the sensitivity for detecting lymph node metastases from 35% when using MRI alone to 90% [18]. However, the reading of this technique is time-consuming, since a node-by-node comparison must be made between the native MRI and a second MRI after contrast agent, and requires special expertise. Moreover, it cannot overcome the problem of false-negative normal-sized LN harbouring micrometastases. Besides, recent studies have been conducted when applying super-paramagnetic particles of iron oxide and Diffusion-Weighted sequence (DW-MRI) [18]. In normal lymph nodes, the uptake of iron oxide particles by macrophages produces a signal decrease on T2/T2*-weighted magnetic resonance sequences, so improving diagnostic accuracy. The combination of two effects (reduced diffusion together with relatively unchanged T2/T2* after USPIO in malignant lymph nodes) leads to hyperintense signals and thus to a possibly better separation from normal lymph nodes, which are supposed to become invisible due to reduced T2/T2*. Unfortunately, these agents are not yet available in the daily clinical

practice [19]. For lymph node evaluation, functional MRI, and in particular DW imaging, represents one of the most interesting fields of research.

Diffusion-weighted imaging (DWI) derives its contrast from the regional differences in the mobility of water molecules. The ADC is a quantitative parameter that reflects the diffusion of water and tissue perfusion. DWI has been investigated for use in differentiating benign from malignant lymph nodes in head and neck carcinomas. It has been anticipated that ADC may improve the diagnostic performance of MR in the detection of metastatic lymph nodes on the basis of a lower ADC value in cancer tissue than in non-cancerous tissue. Moreover, only small groups of patients have been investigated and discrepancies exist between different authors [20].

On the basis of our preliminary experience high-quality DW-MRI of lymph nodes should be performed as part of a primary tumour staging without significantly increasing the imaging time. This unique modality can help to distinguish benign from malignant lymph nodes and has achieved promising NPV values in our study group. In addition, the ADC based on DW imaging shows an advantage over CT, MRI and PET since the measurement of the ADC is relatively unrelated to the lesion size if the region of interest is placed inside the lymph node. Recent preliminary studies on patients with head and neck cancers have reported that DWI can depict metastatic cervical lymph nodes from benign lymphadenopathies and nodal lymphomas with a high degree of accuracy [21-22]. All authors have reported significant differences in ADC between

metastatic and normal lymph nodes. However, some discrepancies exist between those different studies concerning the level of ADC value provided. Razek et al. [21] reported that metastatic lymph nodes have lower ADC values than benign lymph nodes. On the contrary, Sumi et al. [22] observed a significant elevation of ADC compared with benign lymphadenopathy. A large spectrum of ADC values among metastatic lymph nodes was presented and can be explained by differences in the cellular composition of tumours. The higher ADC value observed in metastatic nodes can be explained by the presence of a necrotic part that exhibits high ADC values because of the free diffusion of water. The development of fibrous tissue which produced restriction of water diffusion is another potential cause of ADC variation [20]. When comparing ADC values in the literature for any organ and lesion, attention has also to be paid to the choice of the underlying b-value, because the mobility is quantified by calculating the ADC, which depends mainly on the choice of the underlying b-values [17].

However, to ensure accurate nodal assessment, it is important to be aware of the potential pitfalls of DW-MRI imaging and to review findings in conjunction with morphological sequences for anatomical localization and correlation of radiologic findings with histopathology. Potential pitfalls and limitations of DW-MRI for nodal assessment should be borne in mind when applying the technique for evaluation:

1. Small nodes (< 4 mm in long axis diameter) may be visualized using DW-MRI and anatomically localized but the presence of malignant disease cannot be always established using the technique.
2. The ADC measurements of normal-sized lymph nodes may be degraded by partial volume effects.
3. Necrotic areas in neoplastic nodes may lead to false-negative results due to the resultant ADC increase. Necrotic deposits therefore must be excluded.
4. Decrease in nodal ADC value may result from nodal reactive changes.
5. Instrumental factors such as image noise, motion artefacts can lead to systematic or random ADC quantification errors.
6. Micrometastases in smaller lymph nodes with insufficient intra-nodal tumour burden may not impede water diffusion and can lead to false-negative results [2].

Our interest focused on nodal staging (N) because of the crucial prognostic value. Our preliminary results showed that the ADC value of metastatic lymph nodes was significantly lower than that of the non-metastatic lymph nodes with a positive predictive value of 87,5%. As regards as the FSE-MRI analysis, we found a significant difference between the Grading Score in the nodal metastatic group and in the nodal non-metastatic group, but a very low specificity, positive predictive value and diagnostic accuracy were observed. We also noted that the mean diameter (short axis) of the lymph node in the nodal metastatic group was lower than 10 mm ($6,35 \pm 1,54$ mm; range 4-

9mm), that is the standard cut-off reported in the literature for the pelvic lymph nodes [23-24].

However, the fact that this reflects our initial experience should be taken into consideration. In addition, to our knowledge, no other study has specifically investigated nodal metastases in prostate cancer using DW-MRI with the ADC measurement using the multiple b-values sequence. Moreover, a higher field strength (3T versus 1.5T) should allow an increase in spatial resolution and an improved signal-to-noise ratio.

There are some limitations to this study. First, our number of patients and in particular those which with malignant nodes remains relatively low. Second, we recorded only lymph nodes larger than 4 mm in their long axis. Obviously lymph nodes smaller than 4 mm can be malignant too. Third, the major limitation of this work was that it was a station-by-station analysis and not a node-by-node analysis.

In conclusion, the results were encouraging and our preliminary experience with ADC measurements of pelvic lymph nodes of patients with prostate cancer indicated that ADC can help to differentiate metastatic from non metastatic lymph nodes and that it is more accurate than FSE-MRI evaluation alone.

Nevertheless, a number of published studies have testified the potential of the technique and inter- and intra-observer reproducibility of nodal ADC measurements still needs to be determined to ensure that serial comparison of measurements is clinically meaningful [2].

References

- [1]. Heidenreich A, Bellmunt J, Bolla M, et al. EAU Guidelines on Prostate Cancer. Part 1: Screening, Diagnosis and Treatment of Clinically Localised Disease. *Eur Urol*.2011; 59: 61-71.
- [2]. Baert A.L, Reiser M.F, Hricak H, Knauth M, Koh D.M, Thoeny H.C. (Editors) Diffusion Weighted MR imaging. Applications in the body. Springer-Verlag Berlin Heidelberg 2010.
- [3]. Thoeny HC. Diffusion-weighted MRI in head and neck radiology: applications in oncology. *Cancer maging* 2011; 10: 209-14.
- [4]. Ahmed Abdel Khalek Abdel Razek, Sahar Elkammary, Ahmed Saad Elmorsy, et al. Characterization of mediastinal lymphadenopathy with diffusion-weighted imaging. *MR Imaging* 2011; 29: 167-172.
- [5]. Cagiannos I, Karakiewicz P, Eastham JA, et al. A preoperative nomogram identifying decreased risk of positive pelvic lymph nodes in patients with prostate cancer. *J Urol* 2003; 170: 1798-803.
- [6]. Briganti A, Chun FK-H, Salonia A, et al. Validation of a nomogram predicting the probability of lymph node invasion among patients undergoing radical prostatectomy and extended pelvic lymphadenectomy. *Eur Urol* 2006; 49: 1019-27.

- [7]. Briganti A, Karakiewicz P, Chun FK-H, et al. Percentage of positive biopsy cores can improve the ability to predict lymph node invasion in patients undergoing radical prostatectomy and extended pelvic lymph node dissection. *Eur Urol* 2007; 51: 1573-81.
- [8]. Burkhard FC, Schumacher MC, Studer UE. An extended pelvic lymph node dissection should be performed in most patients if radical prostatectomy is truly indicated. *Nat Clin Pract Urol* 2006; 3: 454-5.
- [9]. Wolf Jr JS, Cher M, Dall'era M, Presti Jr JC, Hricak H, Carroll PR. The use and accuracy of cross-sectional imaging and fine needle aspiration cytology for detection of pelvic lymph node metastases before radical prostatectomy. *J Urol* 1995; 153: 993-9.
- [10]. Tempany CM, McNeil BJ, Advances in biomedical imaging. *JAMA* 2001; 285: 562-7.
- [11]. Katz S, Rosen M, MR imaging and MR spectroscopy in prostate cancer management. *Radiol Clin North Am* 2006; 44: 723-34.
- [12]. Schumacher MC, Burkhard FC, Thalmann GN, Fleischmann A, Studer UE. Good outcome for patients with few lymph node metastases after radical retropubic prostatectomy. *Eur Urol* 2008; 54: 344-52.
- [13]. Barentsz JO, Engelbrecht MR, Witjes JA, de la Rosette JJ, van der Graaf M. MR imaging of the male pelvis. *Eur Radiol* 1999; 9: 1722-36.
- [14]. Dorfman RE, Alpern MB, Gross BH, Sandler MA. Upper abdominal lymph nodes: criteria for normal size determined with CT. *Radiology* 1991; 180: 319-22.

- [15]. Budiharto T, Joniau S, Lerut E, et al. Prospective Evaluation of (11)C-CholinePositron Emission Tomography/Computed Tomography and Diffusion-Weighted Magnetic Resonance Imaging for the Nodal Staging of Prostate Cancer with a High Risk of LymphNode Metastases. *Eur Urol*. 2011 Jul;60(1):125-30.
- [16]. Mattei A, Fuechsel FG, Bhatta Dhar N, et al. The template of the primary lymphatic landing sites of the prostate should be revisited: results of a multimodality mapping study. *Eur Urol* 2008; 53: 118-25.
- [17]. Warncke SH, Mattei A, Fuechsel FG, Z'Brun S, Krause T, Studer UE. Detection rate and operating time required for gamma probe-guided sentinel lymph node resection after injection of technetium-99m nanocolloid into the prostate with and without preoperative imaging. *Eur Urol* 2007; 52: 126-32.
- [18]. Harisinghani MG, Barentsz J, Hahn PF, et al. Noninvasive detection of clinically occult lymph-node metastases in prostate cancer. *N Engl J Med* 2003; 348: 2491-9.
- [19]. Thoeny HC, Triantafyllou M, et al. Combined Ultrasmall Superparamagnetic Particles of Iron Oxide-Enhanced and Diffusion-Weighted Magnetic Resonance Imaging Reliably Detect Pelvic Lymph node Metastases in Normal-Sized of Bladder and Prostate Cancer Patients. *Eur Urol* 2009; 761-769.
- [20]. Roy C, Bierry G, Matau A et al. Value of diffusion-weighted imaging to detect small malignant pelvic lymph nodes at 3 T. *Eur Radiol* (2010) 20: 1803–1811.

- [21]. Razek A, Soliman NY, Elkharaway S, Tawfik A. Role of diffusion-weighted MR imaging in cervical lymphadenopathy. *Eur Radiol* (2006)16:1468–1477.
- [22]. Sumi M, Caunteren MV, Nakamura T. MR micro imaging of benign and malignant nodes in the neck. *AJR Am J Roentgenol* (2006) 186:749–757.
- [23]. Giannarini G, Petralia G, Thoeny H. C. Potential and limitations of Diffusion-Weighted Magnetic Resonance Imaging in Kidney, Prostate and Bladder Cancer Including Pelvic Lymph Node Staging: A Critical Analysis of the Literature. *Eur Urol* 2012; 326-340.
- [24]. Vinnicombe SJ, Norman AR, Nicolson V, Husband JE. Normal pelvic lymph nodes: evaluation with CT after bipedal lymphangiography. *Radiology* 1995 Sep;196(3):800.

Tables

Table 1. D'Amico Risk Groups

| | |
|----------------------------|--|
| HIGH RISK PATIENTS | <ul style="list-style-type: none">• PSA* > 20 or Gleason \geq 8 or are in clinical stage T2c-3a |
| INTERMEDIATE RISK PATIENTS | <ul style="list-style-type: none">• Gleason score of 7 or PSA of 10-20 or are in clinical stage T2b |
| LOW RISK PATIENTS | <ul style="list-style-type: none">• PSA \leq 10ng/ml and Gleason score \leq 6 or are in clinical stage T1-2a |

*PSA** = prostate-specific antigen; ng/ml

Table 2: Grading Score system

| | Point 1 | Point 2 |
|----------------------------------|--------------------|-----------------|
| Intranodal signal intensity (SI) | Homogeneous | Heterogeneous |
| Short axis | $\leq 10\text{mm}$ | $> 10\text{mm}$ |
| Nodal contour | Regular | Irregular |
| L/S Ratio | ≥ 2 | < 2 |

Table 3: Localization and number of lymph nodes (n=53) on DWI

| | No |
|-------------------------|----|
| External iliac proximal | |
| Right | 14 |
| Left | 5 |
| External iliac distal | |
| Right | 10 |
| Left | 10 |
| Internal iliac proximal | |
| Right | 1 |
| Left | 0 |
| Internal iliac distal | |
| Right | 0 |
| Left | 0 |
| Obturator | |
| Right | 6 |
| Left | 6 |
| Common iliac | |
| Right | 1 |
| Left | 0 |

Table 4: Demographic and biometric information (patients n=5)

| | |
|---|--------------|
| Patients, N | 5 |
| Age; mean (range) | 67,2 (56-76) |
| Preoperative PSA, mean (range) | 17 (6-35) |
| Biopsy Gleason grade | |
| 6 (3+3) | |
| 7 (3+4) | 3 |
| 7 (4+3) | |
| 8 (4+4) | 1 |
| 9 (4+5) | 1 |
| 9 (5+4) | |
| Dissected lymph nodes, n | 84 |
| Lymph node count, mean (range) | 16,8 (12-23) |
| Dissected nodal stations, n | 46 |
| Metastatic nodal stations, n/N (%) | 7/46 (15) |
| Non-metastatic nodal stations, n/N (%) | 39/46 (85) |

Table 5: Result of Grading Score per nodal stations (n=28) analysis

| Benign LN stations Score | Malignant LN stations Score |
|-----------------------------|--------------------------------|
| 5,33 | 7 |
| 5,33 | 6,5 |
| 6 | 6,25 |
| 4 | 6 |
| 5,5 | 7 |
| 5 | 6,5 |
| 5 | 6 |
| 5 | |
| 5 | |
| 5 | |
| 5 | |
| 4 | |
| 4 | |
| 5 | |
| 5,5 | |
| 5,28 | |
| 6 | |
| 5 | |
| 5 | |
| 5,5 | |
| 4 | |

Table 6: Results of identifiable nodes on DWI (5 patients) (n=53)

| | Histologically metastatic | Histologically benign | P-value |
|-------------------------------------|-------------------------------|------------------------------|---------|
| No. of nodal stations | 7 | 21 | |
| ADC value Mean \pm SD range | 0.796 \pm 0,09 0,71-0,88 | 1,17 \pm 0,25 1,05-1,28 | 0,0008 |

Table 7: The receiver operating curve (ROC) showed the area under the curve (AUC) of 0.96.

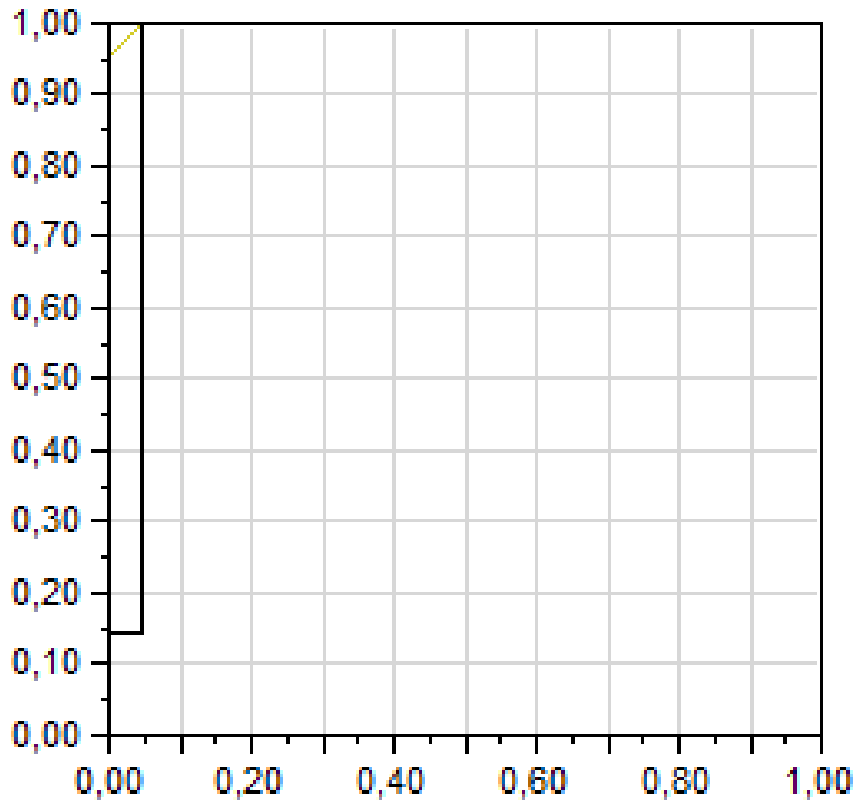


Table 8: Results of MRI according to the apparent diffusion coefficient (ADC) map per nodal stations (NS, n=28) analysis. ADC*: $\times 10^{-3} \text{ mm}^2/\text{s}$

| Benign NS ADC* value | Malignant NS ADC* value |
|-------------------------|----------------------------|
| 1,19 | 0,81 |
| 1,22 | 0,84 |
| 0,64 | 0,91 |
| 1,1 | 0,63 |
| 1,1 | 0,79 |
| 0,96 | 0,83 |
| 1,35 | 0,76 |
| 1 | |
| 1,4 | |
| 0,95 | |
| 1,35 | |
| 1,95 | |
| 1,15 | |
| 1,37 | |
| 1,08 | |
| 1,16 | |
| 1,28 | |
| 1,11 | |
| 1,15 | |
| 1 | |
| 0,98 | |

Table 9: Results of MRI according to the apparent diffusion coefficient (ADC) map per nodal stations (n=28) analysis

| DWI | Histopathology | |
|--|-----------------|-----------------|
| | <i>Positive</i> | <i>Negative</i> |
| $ADC \leq 0,91 \times 10^{-3} \text{ mm}^2/\text{s}$ | 7 | 1 |
| $ADC > 0,91 \times 10^{-3} \text{ mm}^2/\text{s}$ | 0 | 20 |

Figures

Fig. 1: An example of benign lymph node. a. T2w image. b. DW image c. ADC map d. Grading score = 6.

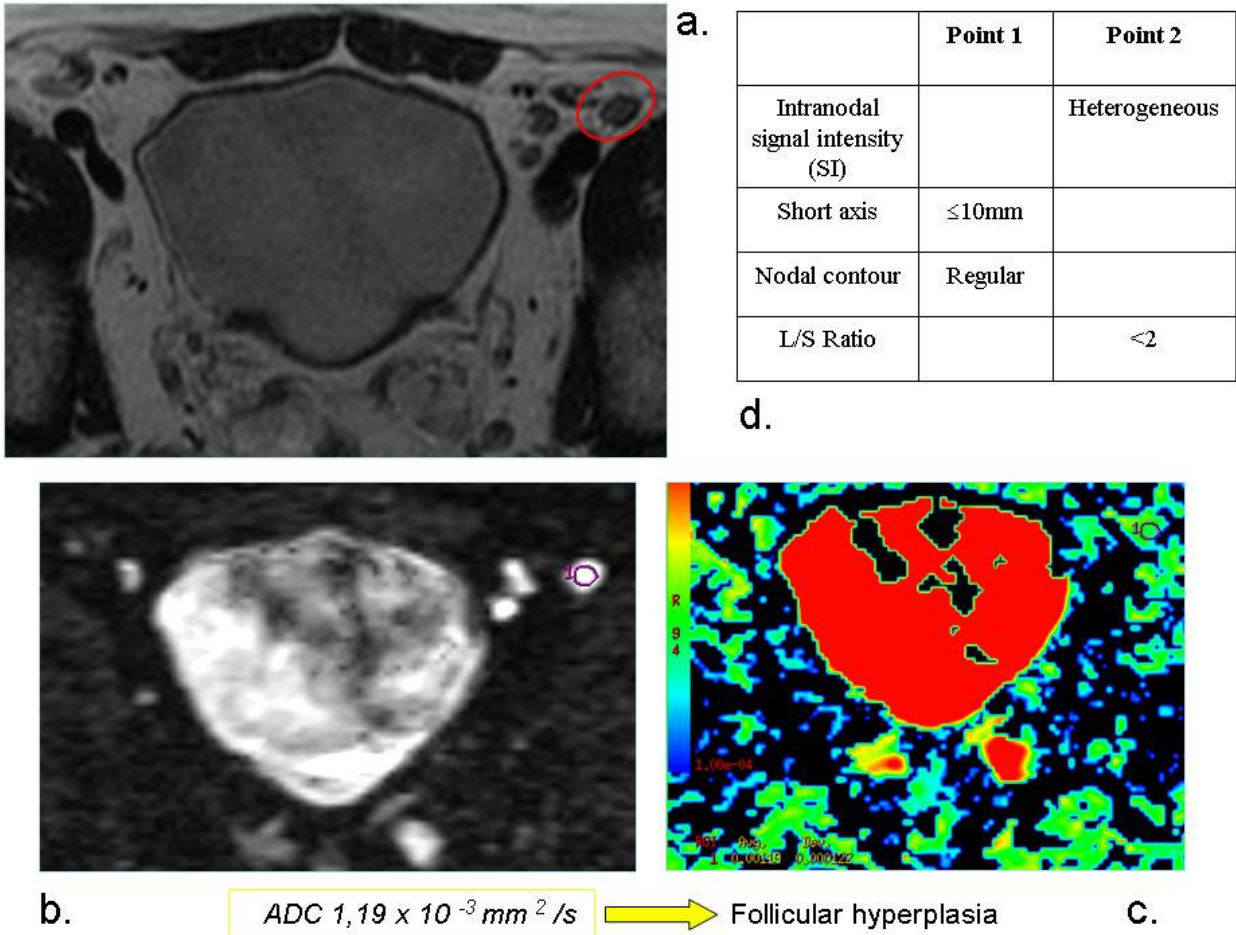
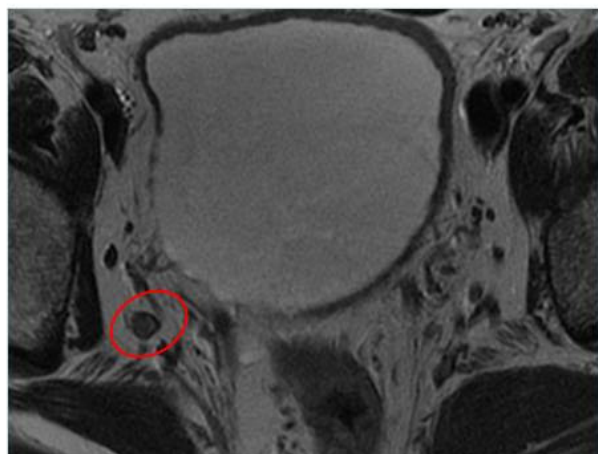


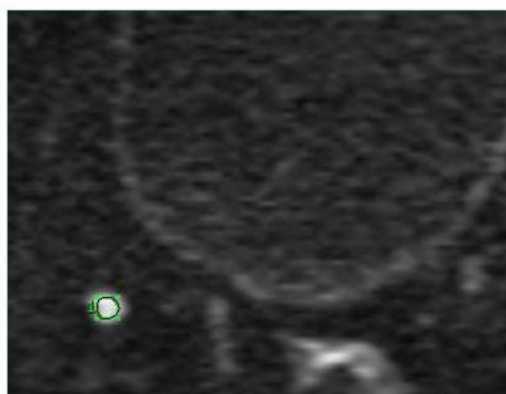
Fig. 2: An example of metastatic lymph node. a. T2w image. b. DW image c. ADC map d. Grading score = 7.



a.

| | Point 1 | Point 2 |
|----------------------------------|---------|---------------|
| Intranodal signal intensity (SI) | | Heterogeneous |
| Short axis | ≤10mm | |
| Nodal contour | | Irregular |
| L/S Ratio | | <2 |

d.

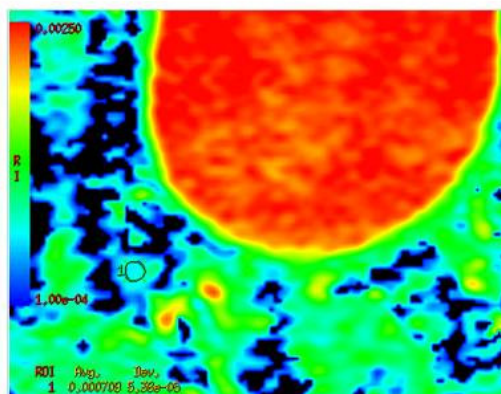


b.

ADC $7,09 \times 10^{-4} \text{ mm}^2/\text{s}$

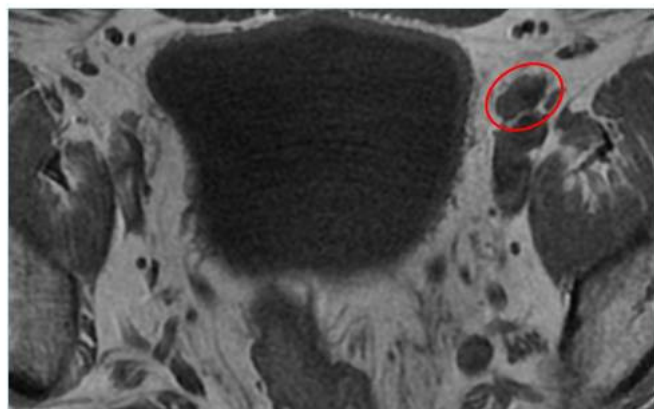


metastatic



c.

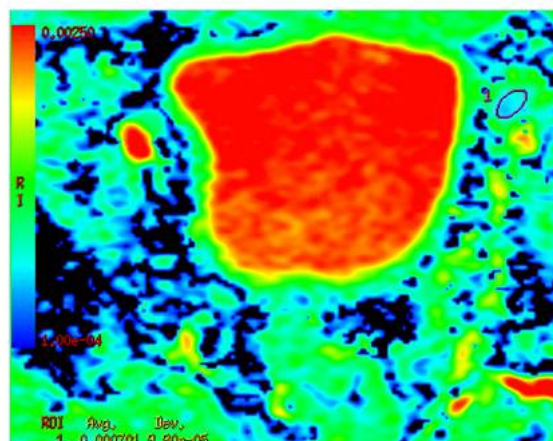
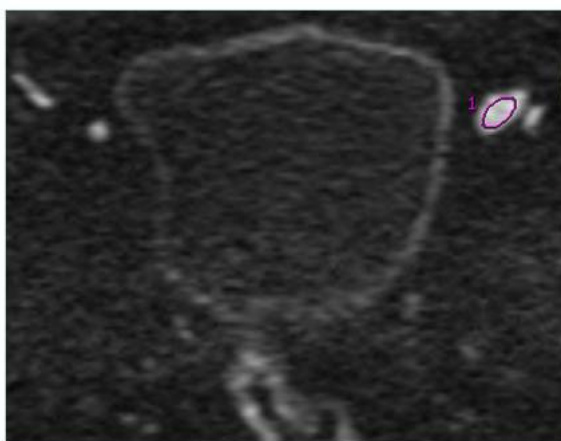
Fig. 3 An example of metastatic lymph node. a. T2w image. b. DW image c. ADC map d. Grading score = 7.



a.

| | Point 1 | Point 2 |
|----------------------------------|---------|---------------|
| Intranodal signal intensity (SI) | | Heterogeneous |
| Short axis | ≤10mm | |
| Nodal contour | | Irregular |
| L/S Ratio | | <2 |

d.



b.

ADC $7,01 \times 10^{-4} \text{ mm}^2/\text{s}$



metastatic

c.